Acta Oceanol. Sin., 2017, Vol. 36, No. 4, P. 37–45
DOI: 10.1007/s13131-016-0918-6
http://www.hyxb.org.cn
E-mail: hyxbe@263.net

Typhoon events recorded in coastal lagoon deposits, southeastern Hainan Island

ZHOU Liang[1, 2], GAO Shu[1, 2*], YANG Yang[1, 2], ZHAO Yangyang[1, 2], HAN Zhuochen[1, 2], LI Gaocong[1, 2]
JIA Peihong[1, 2], YIN Yong[1, 2]

[1] Collaborative Innovation Center of South China Sea Studies, Nanjing 210093, China

[2] Ministry of Education Key Laboratory for Coast and Island Development, Nanjing University, Nanjing 210093, China

Received 19 December 2015; accepted 5 May 2017

Abstract

Coastal lagoon deposits provide evidence for the magnitude and frequency of past tropical cyclones prior to instrumental records and historical documentation. In the present study, we attempt to analyze the sedimentary records containing typhoon information for the northern South China Sea region. For this purpose, sediment cores were collected from two coastal lagoons in the southeastern Hainan Island, and were analyzed in laboratory to derive the data sets about grain size, organic and inorganic carbon contents, and deposition rates. The grain size and organic-inorganic carbon data were used to formulate the proxies of typhoon events. The deposition rates, as calculated using the CRS ^{210}Pb method, are around 0.5 mm/a for both lagoons, on the basis of which an age model is established. Within the cores, sedimentary layers associated with 35 typhoon events have been identified. On such a basis, a 350 year history of local typhoon activities is reconstructed by incorporating the ^{210}Pb dating results, typhoon-induced sedimentation patterns and the historical documents. A comparison of the frequency of typhoon occurrence with the regional climate records indicates that the observed changes in tropical cyclone activity patterns, as revealed by the lagoon sedimentary records, may be related to El Niño, Pacific Decadal Oscillation (PDO), North Atlantic Oscillation (NAO), sunspot, and other potential climate drivers that affect the tropical cyclone variability. This study demonstrates that the sedimentary record of storms can be analyzed in combination with historical documents, to provide meaningful information on past storm activities and their long-term variability.

Key words: paleostorms, typhoon-induced deposits, grain size, loss on ignition, Hainan Island

Citation: Zhou Liang, Gao Shu, Yang Yang, Zhao Yangyang, Han Zhuochen, Li Gaocong, Jia Peihong, Yin Yong. 2017. Typhoon events recorded in coastal lagoon deposits, southeastern Hainan Island. Acta Oceanologica Sinica, 36(4): 37–45, doi: 10.1007/s13131-016-0918-6

1 Introduction

The risk of the coastal zones with catastrophic storm strikes has increased significantly, in response to climate change that modifies the intensity and frequency of storm disasters, and the concentration of the population, urbanization and social wealth in the coastal areas (Emanuel, 2005; Landsea, 2005; Wu et al., 2005; Fan and Liu, 2008; Vecchi and Villarini, 2014). Instrumental records of landfalling typhoons, however, are only available for a period shorter than 100 years in China. The lack of long-term records along the China coastlines limits their use as a suitable data set for systematic analyses. Thus, any knowledge of past storm events will be valuable in the evaluation of potential regional hazards, in terms of regional planning and coastal defense schemes.

Palaeotempestology is the study of prehistoric tempests or storms by means of geological and archival techniques (Liu et al., 2001; Murname and Liu, 2004; Fan and Liu, 2008). It is a relatively young research field which is, however, one of the hottest focusses in global change studies, with an emphasis on the frequency of prehistoric tropical cyclones along the coastlines of, e.g., the southeastern United States (Liu and Fearn, 2000; Collins et al., 1999; Donnelly et al., 2005, Donnelly and Woodruff, 2007; Wallace and Anderson, 2010; Hodges and Elsner, 2011), tropical Australia (Hayne and Chappell, 2001), and to a lesser extent the South China Sea (Yu et al., 2009, 2012). Pre-instrumental tropical cyclone activities can be identified by geological and archive analyses. Historical documents are outstanding in their high spatial precision and temporal resolution, but shorter in time span than geological records and often lack important information due to the various social disturbances (e.g., wars) (Liu and Fearn, 2000; Fan and Liu, 2008). The history of past typhoon activities may be reconstructed by means of reliable sedimentological proxies (such as wash-over deposits preserved in the sediments of coastal lagoons and marshes, beach ridges and cheniers, and storm deposits in atoll lagoons), on the basis of sedimentary organic geochemical properties, and stable isotopic indicators (Liu and Fearn, 2000; Fan and Liu, 2008). Previous studies have shown that low-energy coastal depositional settings, such as lagoons, can offer favorable environments for the preservation of storm-induced deposits (Liu and Fearn, 2000; Donnelly and Woodruff, 2007; Sabatier et al., 2008; Wallace and Anderson, 2010). During a storm event, the normal lagoon sequences may be disturbed by enhanced typhoon-generated waves and storm surges. The sedimentary layers representing such disturbances can be used to reconstruct the typhoon-induced storm events.

The Hainan Island is one of the regions where the coast is fre-

Foundation item: The National Natural Science Foundation of China under contract No. 41530962.
*Corresponding author, E-mail: shugao@nju.edu.cn

quently and seriously affected by tropical storms in the northwestern Pacific margin. The typhoon hitting the island is characterized by high intensity, long duration and frequent occurrence, known as "the corridor of typhoons" (Chen, 1992). However, little is known about the long-term records within the storm-induced deposits, and there is a lack of an understanding of the geographic and temporal controls on the cyclone activity over the northern South China Sea region. With few tsunami events, according to historical documents (Wen, 2007; Chen, 1995), and the presence of a large number of coastal lagoons and salt ponds (Song, 1984), Hainan Island is an ideal area to generate unique deposits during typhoon events. Hence, the purpose of this study is to reconstruct the history of typhoon activities by analyzing coastal lagoon deposits and comparing the results with historical documents for southeastern Hainan Island, and evaluate the relationship between typhoon landfall frequencies and palaeo-climate records.

2 Study areas

The Hainan Island, the second largest island in China, is separated from the mainland by the narrow Qiongzhou Strait (Fig. 1). The island has a staircase-like topographic feature, descending step by step from towering mountains to flat tablelands and plains at its periphery. This island covers an area of 33 900 km^2 with a coastline of 1 725 km in length (Song, 1984). The oceanographic conditions on its southeastern coast are characterized by micro-tides, irregularly diurnal in character. Here, the climate for the coastal region is generally tropical monsoonal, with a dry season from November to April and a wet season from May to October. Typhoons and tropical cyclones from the western Pacific Ocean and the South China Sea frequently hit the southeastern coast of Hainan Island from July to October (Wang et al., 2001). During typhoon events, the accompanied high wind speeds, large storm surges and waves often cause serious damage to the coastal infrastructure and residential areas. The water level associated with storm surges can reach up to 5 m above the mean sea level during strong typhoons (Wang et al., 2001). From 1945 to 2000, the highest storm water level increase was 2.73 m above normal water level, which was recorded in the Xincun Lagoon during the No. 8105 typhoon in 1981 (Chen, 1992).

The Xincun Lagoon is one of the largest lagoons in the southeast of Hainan Island, covering an area of around 22 km^2. The lagoon landforms were formed during the Holocene transgression process. Near the entrance to the lagoon, granite hills (i.e., Nanwan Monkey Island and Liuliang Hill) separate the lagoon from the open sea. The entrance channel is about 3.5 km in length and 260 m in width (Song, 1984). Riverine sediment input into the lagoon is small because only two small streams discharge into the lagoon, with an average flow of around 1 m^3/s. The seabed sediment in the lagoon is generally dominated by fine-grained materials, with sands being mainly distributed near the shoreline.

The Li'an Lagoon, adjacent to the Xincun Lagoon, is connected to the open sea through a small inlet (~60 m in width) (Jiang et al., 2009). It has an area of approximately 8.69 km^2 with an average depth of 5.5 m (the datum being the mean sea level), and a maximum tidal range of 1.5 m (Jiang et al., 2009). Freshwater flow into the lagoon is minimal because the drainage area is too small. To the east and south of the lagoon, large sand barriers divide the embayment from the open sea (Fig. 1). The height of sand barrier is about 8–12 m in the east, and about 6–8 m in the south of the

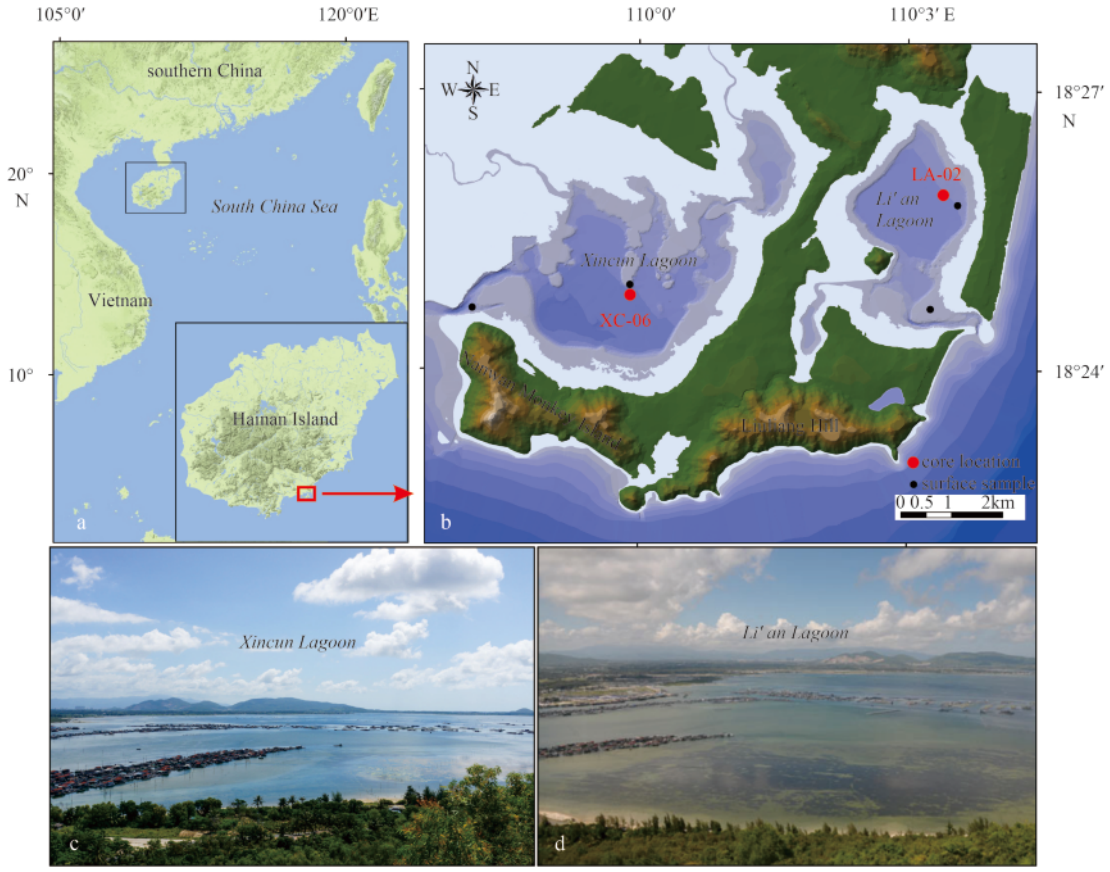

Fig. 1. The environmental setting of the study area: location of Hainan Island (a); sample sites (b); the Xincun Lagoon (c); and the Li'an Lagoon (d).

lagoon, above the mean sea level. The sediment in the Li'an Lagoon is similar to that of the Xincun Lagoon (Song, 1984; The compile committee of China bay records, 1999).

3 Materials and methods

Two cores were collected from the Xincun and Li'an Lagoons, respectively, in August 2013 (for the core sites, see Fig. 1). The position of the cores was fixed using a handheld GPS in the field. Core XC-06 was located at the center of the Xincun Lagoon with a length of 120 cm, and Core LA-02 was collected in the northeastern Li'an Lagoon, with a length of 170 cm. The two cores both consist of olive grey clay silt, interbedded with relatively thick (1–4 cm) coarser-grained sediment layers. These layers are mixtures of olive grey clay silt with coarser grains (i.e., coarse sand to dark gray gravel) and, occasionally, marine shell debris. At the same time, surficial samples were collected along the nearby shorelines and within the entrance to the lagoon (Fig. 1). The cores were cut into halves in the laboratory. One half of each was sliced in 2 cm intervals for loss on ignition analysis, and the other half was further sliced, at 1 cm intervals, for grain size and ^{210}Pb dating. The surficial sediment samples and core sub-samples were stored in a freezer at –20°C. Subsequently, the selected core sub-samples were grounded and sieved through a 0.074 mm sieve in the laboratory before the measurement of ^{210}Pb activity.

Dating with ^{210}Pb was performed in sediment cores by using the constant rate of supply (CRS) model. To estimate the sedimentation rate, total ^{210}Pb was determined by alpha spectrometry through its granddaughter ^{210}Po, assuming secular equilibrium. ^{210}Po and ^{209}Po (yield tracer) were spontaneously deposited onto a nickel disc which was counted on a standard silicon surface barrier detector. ^{210}Pb chronology was determined by using a constant flux and rate model (Goldberg and Koide, 1963).

The analysis of loss on ignition (LOI) follows the standard procedures (Heiri et al., 2001; Wünnemann et al., 2006), to determine organic carbon (at 550°C) and inorganic (at 880°C) carbonate contents of each of the samples, after drying at 105°C for 3 h. Replicate samples had a typical precision of less than ±10%, which acceptable for the method. Grain-size analysis was conducted for the 1-cm sub-samples using a Mastersizer-2000 laser analyzer, with a relative error of below 1% for replicated measurements. Grain-size parameters were calculated by the moment method (McManus, 1988). At the same time, sub-samples at 1-cm spatial resolution were heated at 40°C for 48 h, and the coarse material were separated using a standard 125 μm sieve.

4 Results

4.1 *Identification of storm deposits*

Grain-size distributions are widely used as an environmental indicator, e.g., for distinguishing storm deposits from other sedimentary sequences. Here, a simple method developed by Boulay et al. (2002) is used to determine the grain size classes that had the most significant variation through time (Sun et al., 2003). Standard deviation value vs. grain size classes of Cores XC-06 and LA-02 are displayed in Fig. 2. Two main grain populations, representing those with the highest variability, can be identified. One occurs between 4 and 20 μm (clay to fine silt), and another coarser one occurs between 450 and 850 μm (coarse sand). The sand-carrying ability increases with flow velocity; thus, coarser sediments may represent the influx of sedimentary materials stirred up by stronger flows. Thus, coarse sand size particles (>125 μm) were used here to distinguish high-energy event deposits.

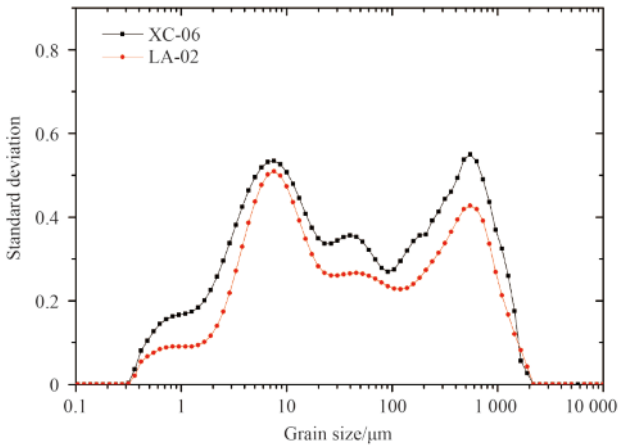

Fig. 2. Standard deviation curves for different grain-size classes.

Cores XC-06 and LA-02 both show significant coarse grain size variations within the coarse-grained layers (Fig. 3). These layers are characterized by poor sorting, negative skewness and the presence of marine shell fragments. They are very different from the underlying and overlying sediments.

Grain size distribution and statistical indices of the surface sediments and coarse-grained layers in Core XC-06 and Core LA-02 are shown in Fig. 4 and Table 1. The surficial sediment was very different from coarse-grained layers sediment (62 cm, 74 cm, 53 cm and 112 cm), but was similar to the sediments in the near shore area adjacent to the core location. The curve of the surficial sediment shows a significant single peak shape between 4 μm and 20 μm, representing the typical lagoon sediments. All coarse-grained layers (e.g., 62 cm, 74 cm, 53 cm and 112 cm) in XC-06 and LA-02 contain a significant high peak in their coarser grain part of grain-size distribution that was very different from their surface samples. The particle size indices, such as mode (*Md*), mean (*Mz*), skewness (*Sk*), kurtosis (*Kg*) and sorting (*S*) values also differentiate the coarse-grained layers and surface sediments well in XC-06 and LA-02 (Table 1). As indicated elsewhere, the frequency of particle size distribution has been used as a major proxy in the study of marine high-energy event deposition (Donnelly et al., 2005; Donnelly and Woodruff, 2007; Sabatier et al., 2008).

There were significant differences in organic and carbonate concentrations at these coarse-grained layers, with the relative low values in organic matter (OM) and high values in carbonate concentrations (TIC) (Fig. 3), such as at the depth of 62 cm (LA-02), 74 cm (LA-02), 54 cm (XC-06), 112 cm (XC-06). These results suggest that sedimentary environment drastic changes occurred in these layers. It was also found elsewhere that variations in organic and carbonate concentrations in coastal depositional sequence are closely related to changes sedimentary environment (e.g., Liu and Fearn, 2000; Ge et al., 2003; Jia et al., 2012).

The normal lagoon depositional types are often divided into two categories which account for different transport and deposition processes, i.e., fine-grained material carried in suspension form under normal condition, and sandy material transported during a high energy event (e.g., storms). The grain size characteristics of these coarse-grained layers show abrupt changes, with grain size parameters associated with coarsening, worse sorted and more negatively skewed values. In addition, these layers show low organic content and mixture with much shell frag-

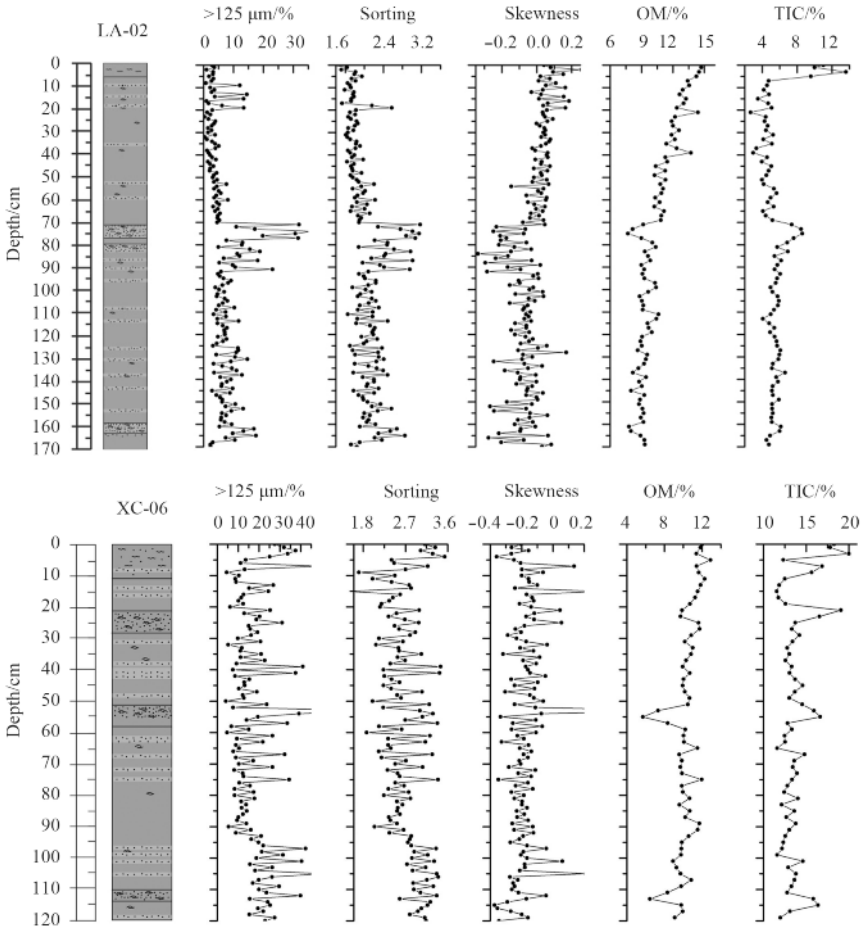

Fig. 3. Vertical variations in grain size and organic matter and carbonate contents, in Cores LA-02 and XC-06.

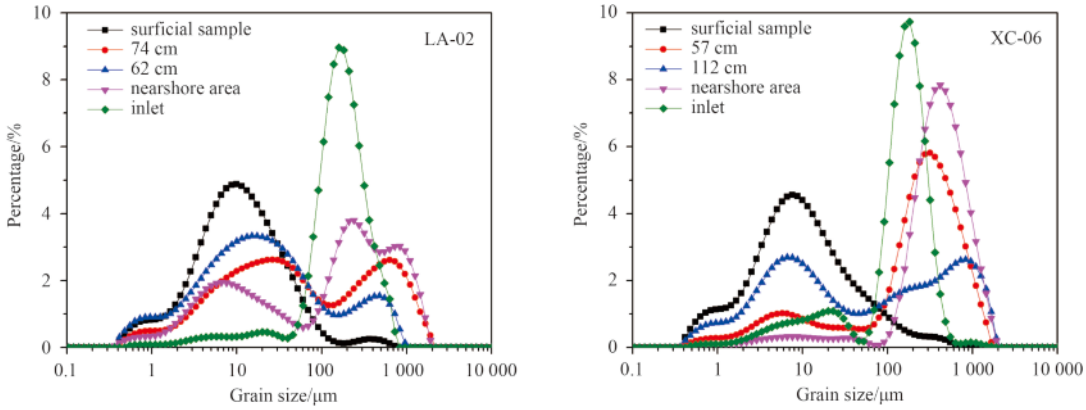

Fig. 4. Grain size frequency curves of sediments in the Li'an and Xincun Lagoons.

Table 1. Grain size parameters of storm layers and surficial sediments

Sample	Mean (*Mz*)/μm	Mode (*Md*)/μm	Skewness (*Sk*)	Kurtosis (*Kg*)	Sorting (*S*)
LA-02-62 cm	12.57	13.27	0.05	1.13	2.05
LA-02-74 cm	57.70	46.80	–0.08	0.76	3.01
Surficial sample (LA)	10.69	10.63	0.03	1.11	1.78
Inlet (LA)	175.70	177.40	0.21	1.71	1.24
Nearshore area (LA)	108.40	202.30	0.39	0.71	3.07
XC-06-57 cm	282.80	966.60	0.80	0.97	3.01
XC-06-112 cm	51.19	46.35	–0.04	0.68	3.37
Inlet (XC)	115.80	166.00	0.55	2.03	1.67
Nearshore area (XC)	397.70	412.10	0.31	1.91	1.37

ments. These observations indicate that the coarser-grained materials were transported as saltation load by high-velocity flows and deposited in a high-energy event environment.

4.2 *Accumulation rate and age model*

The total ^{210}Pb specific activity profile showed an approximately exponential behavior in both Cores XC-06 and LA-02. Sharp gradients in the activity of ^{210}Pb are present at the depths of 65 cm and 60 cm for the sediment Cores XC-06 and LA-02, respectively (Fig. 5). Below the depth at which the sharp changes were found, the ^{210}Pb activity remained almost steady, representing the background value. The sedimentation rates derived by the CRS model indicate that the average sedimentation rate was 5.1 mm/a for XC-06 and 0.475 mm/a for LA-02, respectively. Sediment dates were calculated for the two cores as follows:

$$T = \lambda^{-1} \ln (A_0/A_h), \quad (1)$$

$$S = Z/T, \quad (2)$$

where A_0 is the unsupported ^{210}Pb inventory (Bq/cm^2) of the entire core, A_h is the unsupported ^{210}Pb inventory (Bq/cm^2) beneath sediments of depth h, λ is the ^{210}Pb decay constant (λ= 0.031 14/a), S is the average sedimentation rate (mm/a), T is the age (a) of sediment layers, and Z is the depth (cm) of sediment layers. Dating sediment cores from shallow lakes using ^{210}Pb can be problematic due to the near-instantaneous sedimentation of coarse-grained high-energy event deposits. However, most of the lagoon cores of the Hainan Island have well-defined declines in ^{210}Pb activity (Ge et al., 2003; Liu and Ge, 2012; Jia et al., 2012). These sedimentation rate obtained from this study are in agreement with those previous results in the same area (Ge et al., 2003; Liu and Ge, 2012; Jia et al., 2012). Thus, the ^{210}Pb dating results and sedimentation rate obtained from this study are relatively reliable. Base on the modern average sedimentation rate and the length of the two cores, the periods of XC-06 and LA-02 would be

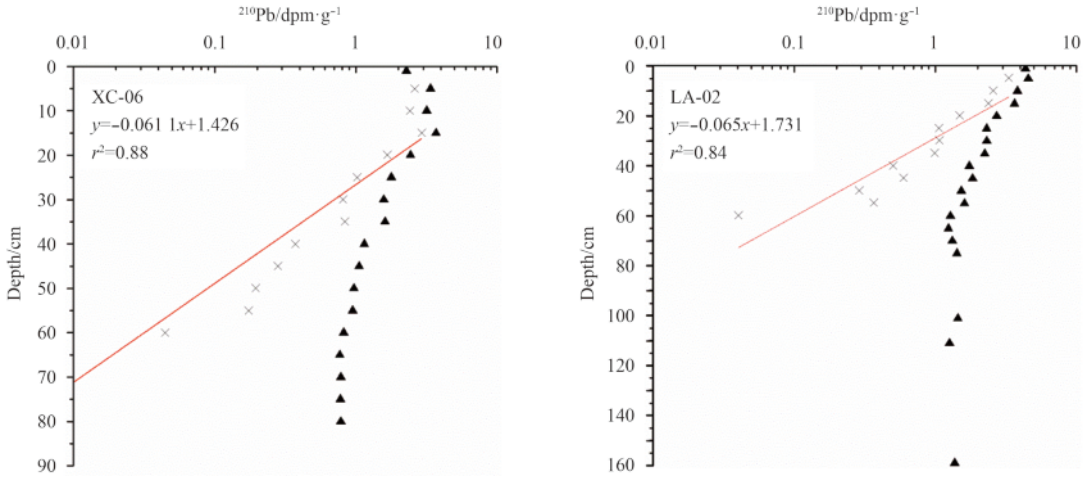

Fig. 5. Profiles of ^{210}Pb activity (▲) and excess ^{210}Pb activity (×) of the sediment cores.

estimated to 235 and 358 years, respectively.

4.3 *The formation of coarse-grained layers*

Investigating the origin of the coarse-grained material offers a possible way of identifying their proximate cause. These deposits may originate from any of the surrounding areas with coarse grains, i.e., near-shore areas, watershed sediment and/or that of the sandy beach during high-energy marine flooding events. For example all coarse-grained layers analyzed in LA-02 contain a mode in their grain size distribution between 450 and 850 μm that was very likely source from the near-shore areas to the east given the modern distribution of grain size observed in this setting (Fig. 4). Similar coarse grain layers of Core XC-06 at 57 and 112 cm also contain a peak between 450 and 850 μm that are likely derived from the sediment from near-shore areas to the west near the core location or tidal inlet area (Fig. 4). Being coarser, worse sorted and more mineral-rich, the coarse-grained layers in the two layers are a better match with the near shore areas sediments. Although the present analysis is limited by characterization of modern grain size, there look like similarities between individual peaks within the multimodal distribution of these coarse-grained layers and grain size distribution of the nearshore areas.

The coarse-grained layers are likely deposited by high-energy event environment. Although tsunamis offer a possible alternative high-energy source for the deposition, there is no historical documents records from this area during the past 500 years. Rain events related to tropical cyclones can explain for the deposition, however, they also cannot the possible causative agent. Not only the long distance between the stream mouths and the core locations, but also the weak runoff of these streams. Therefore, the most likely explanation for the sedimentary signature of coarse-grained layers is extreme tropical cyclones. Storm surge can dramatically raise the water level inside the small sub-bays by funneling the sea water through the tidal channels of the two lagoons. The sediment load should increase due to both the transport of eroded nearshore or nearby beach coarse-grained material and the resuspension of bay sediments. The suspended sediments, consisting of the fine-grained materials resulting from resuspension within the embayment and the coarse-grained material from eroding nearshore areas or beaches, are anticipated to accumulate on the sea bottom of the two lagoons.

5 Discussion

5.1 *Identification of paleostorms*

Southern Hainan Island coastlines adjacent to Sanya City, Lingshui County and Wanning City are frequently and severely

affected by tropical storms (Chen, 1992, 1995; Wen, 2007). It has a long history of documenting the weather and climate phenomena. The documentary archives with paleostorm information can be traced back to the Song Dynasty (AD 960–1279) and the Yuan Dynasty (AD 1271–1368), and the time series of climatic descriptions were almost uninterrupted in the last 500 years (Chen, 1995; Wen, 2007). These data have been compiled partly as an important chapter in various books of natural disaster or meteorological record collections (Chen, 1995; Wen, 2007). ^{210}Pb dating results correlation with the historical accounts are used to reconstruct the history of paleostorm activities during the past 350 years.

The above analytical results show that >125 μm grain size peaks correspond very well to the storm event layers. Both laser grain size analysis and wet sieve analysis were used to accurately identify every storm event layers. Figure 6 shows that the >125 μm grain size curves obtained by both two methods are basically identical. However, the curve obtained from the wet sieve analysis is shift more significant changes at these coarse-grained layers. Thus, the >125 μm grain size peaks obtained by wet sieve analysis is more representative of paleostorm event layers. It is clear that typhoons have been very frequent in the last 350 years. During this time, typhoons occurred 1 or 2 times every 10 years. Figure 6 shows that >125 μm grain size peaks correspond very well to southern Hainan Island typhoons since AD 1660 as shown by Chen (1995) and Wen (2007). For example, at about AD 1994, 1985, 1981, 1973, 1940, 1901, 1886, 1863 of Core LA-02, the >125 μm grain size peaks are consistent with the extreme flooding events recorded in the southeast of the Hainan Island in AD 1994, 1985, 1981, 1973, 1941, 1900, 1890, 1863 (Chen, 1995; Wen, 2007). Similarly, at about AD 2000, 1988, 1984, 1972, 1964, 1945, 1937 of Core XC-06, the >125 μm grain size peaks are also consistent with the extreme flooding events recorded in southeast Hainan Island for the years of AD 2000, 1989, 1985, 1973, 1964, 1944, 1934 (Chen, 1995; Wen, 2007). It is worth noting that, during the period of AD 1902–1910, >125 μm grain size peaks reached its maximum in the 350 year typhoon records, have a good correspondence with four times typhoon events in historical documentary records in period of AD 1906–1909. Thus, the significant high >125 μm grain size peaks in the two cores may represent the result of several typhoon events. It should be noted that the most recent extreme typhoon events were not recorded in the studied cores since 2000, which may reflect the impacts of human activities in the study area. The chronology of every storm events were obtained by comparison ^{210}Pb dating results and historical accounts. Base on this age model, there were 35 times of storm events recorded in the two cores. However, some historical typhoon records do not correspond to our results. Possible reasons for these discrepancies may be that the historical typhoon years have been omitted, or the scales of typhoons were so small that they were not compiled in the literature. Due to the lack of typhoon event sediment records in some of those periods, we could only obtain typhoon-years from the historical records.

However, the chronological sequence of storm events recorded in the two cores was not completely inconsistent. The likely explanation is that the prevailing wind direction of typhoons may be difference because of different landfalling locations. If the typhoon landed to the north of the study area, the nearshore

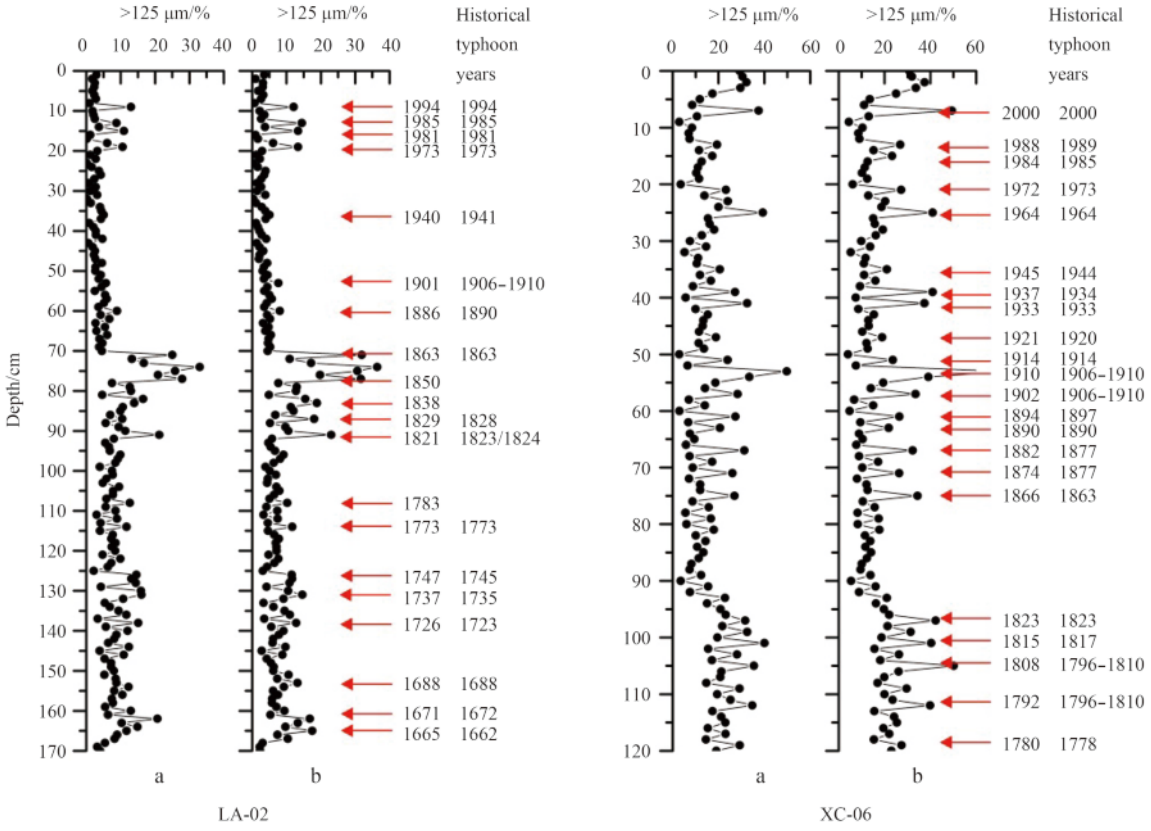

Fig. 6. Comparison of the paleostorm event timing between sedimentary records and historical documents. 125 μm grain size curves obtained by laser grain size analysis (a) and wet sieve analysis (b). The red arrows indicate the paleostorm events recorded in both sediment cores.

coarse-grained materials more likely be eroded and deposited at the location of LA-02 under the influence of westerly or northerly winds. Likewise, when the typhoon landed to the south, the nearshore or nearby beach coarse-grained materials more likely be eroded and deposited at the location of XC-06 under the influence of southerly or easterly winds. In 1964, for example, the storm sediment record only preserved in XC-06 is most likely due to all of severe typhoons landed to the south and the prevailing easterly winds during typhoon sweeping the study area.

The coarse-grained event deposits have a good correspondence with historical extreme storm documentary records of southeastern Hainan Island. Although we have not studied a multi-transect cores, the record analysis of storm event deposits from the near shore area provided evidence of main typhoons in the last 350 years in the southeast of Hainan Island.

5.2 *Linkage between paleostorm activity and atmospheric circulation*

In recent years, although there is a large uncertainty in the trends of typhoon frequency under a warmer climate, researches had made a series of significant progresses (Shi and Zhou, 1990; He, 1999; Chan, 2000; Wu et al., 2004; Wang et al., 2007; Goh and Chan, 2010). Previous studies have reported that observed annual tropical cyclone totals in the western North Pacific are virtually correlated with El Niño-Southern Oscillation (ENSO) Pacific, Decadal Oscillation (PDO), North Atlantic Oscillation (NAO), subtropical high of Atlantic, sea surface temperatures and sunspot activity (Wu et al., 2004; Wang et al., 2007; Zhou et al., 2008; Goh and Chan, 2010; Hung, 2013; Zhou and Cui, 2014). Currently, few continuous multi-centennial records of tropical cyclone activity exists for the northern South China Sea, however, the lagoon sediment records from this region provide key insight into past tropical cyclone activity. Base on the typhoon evidence of sediment records and historical documents, the composite storm frequency was established to compare with these climate records.

Many studies have revealed that tropical cyclone frequency in the western North Pacific is negatively associated with EN (El Niño) years, but positively associated with LN (La Niña) years (He, 1999; Chan, 2000; Wu et al., 2004; Goh and Chan, 2010). However, statistical analyses of the typhoon frequency since AD 1884 in the western North Pacific indicated that there were no significant differences in typhoon frequency between the EN years and LN (La Niña) years (He, 1999). A comparison number of tropical cyclones per year with ENSO indices indicate that the total number of tropical cyclones is not significantly correlated with ENSO, but more intense typhoons appeared in EN years (Camargo and Sobel, 2005). Figure 7 shows that the frequency of extreme storm in the southeastern Hainan Island is high positively associated with Niño3.4 during the past 350 years, especially in the periods of 1740–1755, 1770–1780, 1820–1830 and 1875–1925. Possible reason is that typhoon generated in the South China Sea presents a trend of westward and southward shift in strong El Niño events, and the western Pacific subtropical

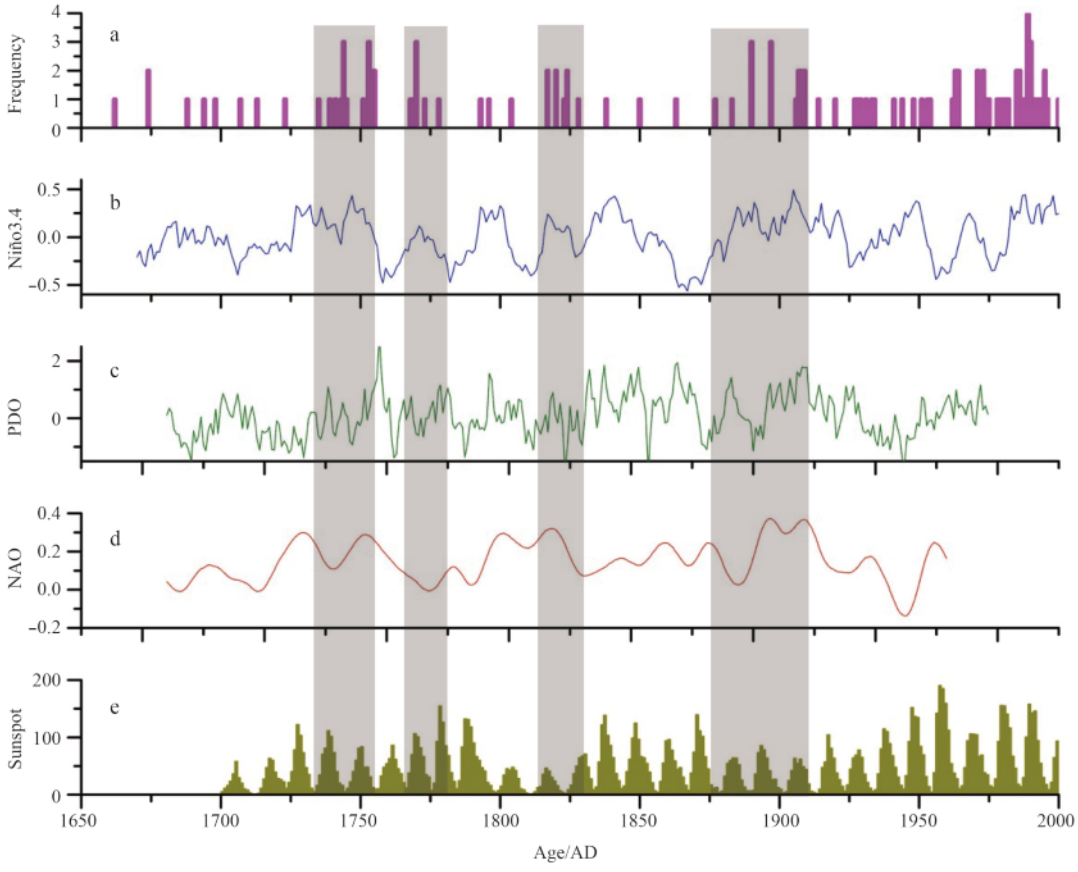

Fig. 7. Time series of paleostorms and circulation factors for the last 350 years in the southeastern Hainan Island: occurrences of paleostorms (a); El Niño index 3.4 with 11-year moving averages (after Cook et al., 2004) (b); Pacific Decadal Oscillation patterns during AD1470–1949 (after Shen et al., 2006) (c); North Atlantic Oscillation patterns with 11-years moving average (after Trouet al., 2009) (d); and sunspot occurrences during AD1700–2000 (from http://sidc.oma.be/silso) (e).

high would westward extension during strong El Niño years (Ruan, 1989; Shi and Zhou, 1990; Wu et al., 2005). This allows a greater number of typhoons from the western Pacific move into the South China Sea, and more typhoons would be generated in the South China Sea (Wang et al., 2007). Another explanation could be that there is an increase in the lifetimes and intensity of tropical cyclones in strong El Niño years, though the number of storms is decreased. Therefore, the extreme typhoon hitting the southeastern Hainan Island would be increases both number and intensity in strong El Niño years.

Figure 7 also shows that fewer typhoons are associated with a positive phase of the Pacific Decadal Oscillation (PDO) and NAO in the study region, while more typhoons favour a negative PDO and NAO phase. One possible explanation is that the number of typhoon hit this region would be more impacted by extreme typhoons from the SCS during the negative PDO and NAO phase. However, the number of typhoon hit this region can be strong influenced by other climatic factors during the positive phase of the PDO and NAO. Their results agreed with the regular patterns of typhoon activities in the SCS, but contrary to the moving regulation of typhoon activities in the northwestern Pacific.

It is worth noting that typhoon counts are significantly related to solar activity (Fig. 7), i.e., there is an inverse relationship between solar activity and typhoon frequency. A possible mechanism for the relationship is that more intense solar activity can warm the lower stratosphere and the upper troposphere through absorption of additional ultraviolet (UV) radiation (Elsner and Jagger, 2008). This would reduce the maximum potential energy and therefore decrease the frequency of typhoon occurrence. The correlation analysis, such as in the periods of 1820–1830 and 1875–1925, is repeated with similar results using data from historical documents at the Taiwan Island (Hung, 2013). Thus, the solar activity has a significant impact on the TC activity along the coastal areas of northwestern Pacific.

There is a decrease trend of typhoon frequency during the period of 1830–1875, though the intensity of Niño3.4 also tends to decrease. The likely explanation is that the typhoons will decreases with increasing solar activity, the negative NAO, and the negative PDO phase would further count against the formation of typhoon in the northwestern Pacific. Additionally, the activity of typhoons that affect the southeast Hainan Island in particular could also be due, to some extent, to other influences, e.g., sea surface temperature and East Asian summer monsoon (Wang et al., 2008).

6 Conclusions

The study of the Xincun and Li'an Lagoons shows that analyses of sedimentology, geochemistry and historical archives allow the identification of the major storm events in the southeastern Hainan Island. Within the cores, sedimentary layers associated with 35 typhoon events have been identified. Average sedimentation rates calculated by using the CRS ^{210}Pb method are 4.75 mm/a and 5.1 mm/a for both cores, respectively. Base on the ^{210}Pb dating results, typhoon-induced sediment records and the historical documents, a 350 year history of local typhoon activities is reconstructed. A comparison of the frequency of typhoon occurrence with the regional climate records indicates that the observed changes in tropical cyclone activity patterns may be related to EI Niño, Pacific Decadal Oscillation (PDO), NAO, sunspot, and other potential climate drivers that affect the tropical cyclone variability. These results provide insight into the history of typhoons events in the northern of South China Sea using new methodology for lagoon settings.

Acknowledgements

This research was supported by the Hainan Provincial Government and the Collaborative Innovation Center of South China Sea, Nanjing University. Wang Yaping, Gao Jianhua and Wuennemann B are thanked for their help with laboratory analysis. The authors would like to thank Ge Chendong and the laboratory colleagues for their help with the field work.

References

Boulay S, Colin C, Trentesaux A, et al. 2002. Mineralogy and sedimentology of Pleistocene sediments in the South China Sea (ODP Site 1144). In: Proceedings of the Ocean Drilling Program, Scientific Results. Texas: Texas A & M University

Camargo S J, Sobel A H. 2005. Western North Pacific tropical cyclone intensity and ENSO. Journal of Climate, 18(15): 2996–3006

Chan J C L. 2000. Tropical cyclone activity over the Western North Pacific associated with El Niño and La Niña events. Journal of Climate, 13(16): 2960–2972

Chen Guangxing. 1992. Typhoons and storms in Hainan Island. Journal of China Hydrology (in Chinese), (5): 52–55

Chen Hansong. 1995. Natural Disasters in Hainan Province during the Past 1000 Years (in Chinese). Haikou: Hainan Press, 1–236

Collins E S, Scott D B, Gayes P T. 1999. Hurricane records on the South Carolina coast: can they be detected in the sediment record?. Quaternary International, 56(1): 15–26

Cook E R, Woodhouse C A, Eakin M C, et al. 2004. Long-term aridity changes in the western United States. Science, 306: 1015–1018

Donnelly J P. 2005. Evidence of past intense tropical cyclones from backbarrier salt pond sediments: a case study from Isla de Culebrita, Puerto Rico, USA. Journal of Coastal Research, 42: 201–210

Donnelly J P, Woodruff J D. 2007. Intense hurricane activity over the past 5,000 years controlled by El Niño and the West African monsoon. Nature, 447(7143): 465–468

Elsner J B, Jagger T H. 2008. United States and Caribbean tropical cyclone activity related to the solar cycle. Geophysical Research Letters, 35: L18705

Emanuel K. 2005. Increasing destructiveness of tropical cyclones over the past 30 years. Nature, 436(7051): 686–688

Fan Daidu, Liu K B. 2008. Perspectives on the linkage between typhoon activity and global warming from recent research advances in paleotempestology. Chinese Science Bulletin, 53(19): 2907–2922

Ge Chendong, Slaymaker O, Pedersen T F. 2003. Change in the sedimentary environment of Wanquan River Estuary, Hainan Island, China. Chinese Science Bulletin, 48(21): 2357–2361

Goldberg E D, Koide M. 1963. Rates of sediment accumulation in the Indian Ocean. In: Geiss J, Goldberg E D, eds. Earth Sciences and Meteoritics. Amsterdam: North Holland Publishing Company, 1: 90–102

Goh A Z C, Chan J C L. 2010. Interannual and interdecadal variations of tropical cyclone activity in the South China Sea. International Journal of Climatology, 30(6): 827–843

Hayne M, Chappell J. 2001. Cyclone frequency during the last 5,000 years at Curacoa Island, north Queensland, Australia. Palaeogeography, Palaeoclimatology, Palaeoecology, 168(3–4): 207–219

He Min, Song Wenling, Chen Xingfang. 1999. Typhoon activity in the northwest Pacific in relation to El Niño and LA Nina events. Journal of Tropical Meteorology (in Chinese), 15(1): 17–25

Heiri O, Lotter A F, Lemcke G. 2001. Loss on ignition as a method for estimating organic and carbonate content in sediments: reproducibility and comparability of results. Journal of Paleolimnology, 25(1): 101–110

Hodges R E, Elsner J B. 2011. Evidence linking solar variability with US hurricanes. International Journal of Climatology, 31(13): 1897–1907

Hung C W. 2013. A 300-year typhoon record in Taiwan and the relationship with solar activity. Terrestrial, Atmospheric and Oceanic Sciences, 24(4): 737–743

Jia Jianjun, Gao Jianhua, Liu Yifei, et al. 2012. Environmental changes in Shamei Lagoon, Hainan Island, China: interactions between natural processes and human activities. Journal of Asian Earth Sciences, 52: 158–168

Jiang Zengjie, Fang Jianguang, Zhang Jihong, et al. 2009. The calculation of tidal water capacity and water exchange characteristic of Lián Lagoon. Natural Science Journal of Hainan University (in Chinese), 27(3): 261–264

Landsea C W. 2005. Meteorology: hurricanes and global warming. Nature, 438(7071): E11–E12

Liu K B, Fearn M L. 2000. Holocene history of catastrophic hurricane landfalls along the Gulf of Mexico coast reconstructed from coastal lake and marsh sediments. In: Ning Z H, Abdollahi K, eds. Current Stresses and Potential Vulnerabilities: Implications of Global Change for the Gulf Coast Region of the United States. Baton Rouge: Franklin Press, 38–47

Liu Xingjian, Ge Chendong. 2012. Spatial and temporal variations of sedimented organic matter in Xiaohai Lagoon, Hainan Island. Acta Oceanologica Sinica, 31(3): 74–86

Liu K B, Shen Caiming, Louie K S. 2001. A 1,000-year history of typhoon landfalls in Guangdong, Southern China, reconstructed from Chinese historical documentary records. Annals of the Association of American Geographers, 91(3): 453–464

McManus J. 1988. Grain-size determination and interpretation. In: Tucker M, ed. Techniques in Sedimentology. Oxford: Blackwell, 63–85

Murname R J, Liu K B. 2004. Hurricanes and Typhoons: Past, Present, and Future. New York: Columbia University Press, 13–57

Ruan Junshi. 1989. Preliminary analysis of strong ENSO and tropical cyclone activity in the Western North Pacific during 1982–1983. Marine Science Bulletin (in Chinese), 8(3): 21–28

Sabatier P, Dezileau L, Condomines M, et al. 2008. Reconstruction of paleostorm events in a coastal lagoon (Hérault, South of France). Marine Geology, 251(3): 224–232

Shen Caiming, Wang W C, Gong Wei, et al. 2006. A Pacific Decadal Oscillation record since 1470 AD reconstructed from proxy data of summer rainfall over eastern China. Geophysical Research Letters, 33(3): doi: 10.1029/2005GL024804

Shi Neng, Zhou Jiade. 1990. A statistical analysis of typhoon activities over the South China Sea and ENSO. Meteorological Monthly (in Chinese), 15(4): 9–14

Song Chaojing. 1984. Geomorphology and the tidal inlets in the East Coast of Hainan Island. Studia Marine Science of South China Sea (in Chinese), (5): 31–50

Sun Youbin, Gao Shu, Li Jun. 2003. Preliminary analysis of grain-size populations with environmentally sensitive terrigenous components in marginal sea setting. Chinese Science Bulletin, 48(2): 184–187

The Compile Committee of China Bay Records. 1999. China Bay Records 11th Fascicule (in Chinese). Beijing: China Ocean Press, 109–130

Trouet V, Esper J, Graham N E, et al. 2009. Persistent positive North Atlantic Oscillation mode dominated the Medieval Climate Anomaly. Science, 324: 78–80

Vecchi G A, Villarini G. 2014. Next Season's hurricanes. Science, 343(6171): 618–619

Wallace D J, Anderson J B. 2010. Evidence of similar probablility of intense hurricane strikes for the Gulf of Mexico over the late Holocene. Geology, 38(6): 511–514

Wang Yongmei, Li Weijing, Ren Fumin, et al. 2008. Study on climatic characteristics of china-influencing typhoons and the interrelations between them and their environmental factors. Journal of Tropical Meteorology, 14(1): 24–27

Wang Ying, Peter M I, Zhu Dakui, et al. 2001. Coastal plain evolution in southern Hainan Island, China. Chinese Science Bulletin, 46(1): 90–96

Wang Huijun, Sun Jianqi, Fan Ke. 2007. Relationships between the North Pacific Oscillation and the typhoon/hurricane frequencies. Science in China Series D: Earth Sciences, 50(9): 1409–1416

Wen Kegang. 2007. Disasters in China—Hainan Province (in Chinese). Beijing: Meteorological Press, 1–281

Wu Manchi, Chang W L, Leung W M. 2004. Impacts of El Niño-Southern Oscillation events on tropical cyclone landfalling activity in the Western North Pacific. Notes and Correspondence, 15: 1419–1428

Wu Liguang, Wang Bin, Geng Shuqin. 2005. Growing typhoon influence on East Asia. Geophysical Research Letters, 32(18): L18703

Wünnemann B, Mischke S, Chen Fahu. 2006. A Holocene sedimentary record from Bosten Lake, China. Palaeogeography, Palaeoclimatology, Palaeoecology, 234(2–4): 223–238

Yu Kefu, Zhao Jianxin, Roff G, et al. 2012. High-precision U-series ages of transported coral blocks on Heron Reef (southern Great Barrier Reef) and storm activity during the past century. Palaeogeography, Palaeoclimatology, Palaeoecology, 337–338: 23–36

Yu Kefu, Zhao Jianxin, Shi Qi, et al. 2009. Reconstruction of storm/tsunami records over the last 4000 years using transported coral blocks and lagoon sediments in the southern South China Sea. Quaternary International, 195(1–2): 128–137

Zhou Botao, Cui Xuan. 2014. Interdecadal change of the linkage between the North Atlantic Oscillation and the tropical cyclone frequency over the western North Pacific. Science in China Series D: Earth Sciences, 57(9): 2148–2155

Zhou Botao, Cui Xuan, Zhao Ping. 2008. Relationship between the Asian-Pacific oscillation and the tropical cyclone frequency in the western North Pacific. Science in China Series D: Earth Sciences, 51(3): 380–385